

Analytical Evaluation of the Cyclic Response of Reinforced Concrete Beam-to-Column Connections



B. Burak

Middle East Technical University, Ankara, Turkey

M. Unal

Pennsylvania State University, University Park, PA, USA

SUMMARY:

The shear distortions that beam-to-column connections undergo under earthquake loading have a major contribution to the story drift of a structure. However, the connection regions are generally modeled as rigid zones and the inelastic behavior of the joint is not considered in the dynamic analysis. Therefore, the story drifts are underestimated and the seismic performance of a building cannot be assessed properly. In this study, a model that predicts the joint shear strength versus strain relationship is developed. First, an experimental database is constructed and the key parameters that affect the joint behavior are utilized to develop the joint model. Then, nonlinear analyses are carried out by using Perform 3D with and without the joint model and the analytical results are compared with the experimental ones. The results indicated that considering the developed joint model improves the prediction of the overall seismic behavior and member responses.

Keywords: Beam-to-column connections, joint shear strength, joint distortion, joint model, seismic loading.

1. INTRODUCTION

The shear distortions observed in beam-to-column connection regions significantly affects the seismic response of reinforced concrete structures. Many experimental and analytical studies have been carried out on the behavior of beam-to-column connections under earthquake loading. The key parameters influencing joint behavior are investigated and joint models are developed to predict the structural behavior more accurately.

Durrani and Wight (1985) observed that the level of joint shear stress and the shear reinforcement ratio are important parameters for the seismic performance. Ehsani and Wight (1985) concluded that the moment strength ratio, joint transverse reinforcement ratio and joint shear stress levels are the key parameters that affect the connection behavior. Raffaele and Wight (1995), Chen and Chen (1999) and Teng and Zhou (2008) observed that eccentric beam-to-column connections have a reduced joint strength and stiffness. Burak (2005), Burak and Wight (2008) and Shin (2004-a) found out that if the floor system is included in the test set up, the effect of eccentricity on the seismic performance becomes negligible.

Ehsani and Alameddine (1991) emphasized the effect of concrete compressive strength on the shear capacity and ductility of the connection regions. Kaku and Asakusa (1991) investigated the effect of axial load on the joint shear strength. When Fujii and Morita (1991) compared the joint behavior of interior and exterior reinforced concrete connections the exterior joints were observed to have less shear strength than interior joint subassemblies.

LaFave and Wight (1999) and Quintero-Febres and Wight (2001) tested wide beam-column-slab subassemblies and concluded that wide beams provide extra confinement to the connection regions. However, Burak and Wight (2008) stated that the depth of the wide beam is an important parameter and shallow beams may not provide sufficient confinement to the connection region.

Based on the experimental studies, the key parameters that affect the connection response are obtained and numerous analytical studies have been conducted to predict the joint shear stress versus strain

response. Parra-Montesinos and Wight (2002) proposed an analytical model for estimating shear strength versus strain response of reinforced concrete beam-to-column connections based on the state of plane strains in the joint. Lowes and Altoontash (2003) developed a joint model by developing constitutive relationships of material, geometric and design parameters and implementing a four-node 12 degree-of-freedom element. Mitra and Lowes (2007) improved this model by changing the element definition using a compression-strut model to simulate the joint core.

Shin and LaFave (2004-b) proposed a joint model to estimate the hysteretic joint shear stress versus strain behavior by employing modified compression field theory. Burak (2005) also developed a joint model that predicts the joint shear behavior considering concrete compressive strength, geometry and eccentricity as the key parameters. Canbolat (2008) developed a parametric joint model that takes into account the material properties, geometric properties and confinement provided by the joint hoop reinforcement. More recently, Kim and LaFave (2008) used statistical methods to evaluate the effect of key parameters and developed an equation representing joint shear strength by using Bayesian parameter estimation approach.

In this analytical study, key parameters that influence the joint shear strength were selected and a database was constructed to investigate the effect of these parameters on the seismic behavior of beam-to-column connections. This database was utilized in the development of an inelastic joint model. Dynamic analyses using this developed model improve the prediction of the lateral load vs. story drift response of the structure and provide information on the inelastic behavior of individual members including the connection region.

2. DATABASE COLLECTION

In the development of the joint model, the first step is to collect a database of experimental studies involving both interior and exterior connections tested under reversed cyclic loading. The database provided in Table 2.1 is formed considering only the key parameters that affect the seismic behavior of the connection region such as concrete compressive strength (f'_c), joint transverse reinforcement yield strength (f_y), joint volumetric ratio for one layer of transverse reinforcement ($\rho_{onelayer}$), effective joint width (b_j), column depth (h_c), eccentricity (e), and axial load (N). Subassemblies with wide beams, slabs and/or transverse beams and specimens that have eccentricity between the centerlines of the beams and the column are also included.

Confinement is a key parameter that is either provided by the transverse reinforcement in the joint or by the transverse beams and slab framing into the connection region. Volumetric transverse reinforcement ratio is computed considering the effective confined volume as the effective volume that contains one layer of joint transverse reinforcement:

$$\rho_{onelayer} = \frac{A_o \cdot l_{eff}}{h_{c, core} \cdot b_{c, core} \cdot s} \quad (2.1)$$

where, A_o : the cross-sectional area of the transverse reinforcement,
 l_{eff} : the total effective length of the lateral reinforcement in the loading direction, which is taken as the summation of the lengths of stirrup legs placed parallel to the loading direction,
 $b_{c, core}$: the width of the column core,
 $h_{c, core}$: the depth of the column core,
 s : the spacing of the transverse reinforcement.

Furthermore, the confinement of the connection region by the adjoining beams is taken into account by a parameter, defined as JT (Joint Type Index). Connection subassemblies investigated in this study are divided into five categories from A to E, and joint types and corresponding joint type index values

based on ACI-ASCE Committee 352 Recommendations for Design of Beam-Column Connections in Monolithic Reinforced Concrete Structures (2002) are given in Fig. 2.1.

Table 2.1. Database of Beam-to-Column Connection Subassemblies

Research Team	Specimen	Joint Type, JT	f_c' (MPa)	f_y (MPa)	b_c (mm)	h_c (mm)	b_b (mm)	h_b (mm)	$N/(A_g f_c')$	e (mm)	$\rho_{onelayer}$ (%) Eq. 1	b_j , ACI 352 (mm)	
Burak & Wight (2005, 2008)	1-S	D	1.25	29.0	441	356	356	203	381	0.053	76	1.251	256
	2-S	D	1.25	39.0	441	534	356	254	457	0.039	140	0.815	307
	3-S	D	1.25	29.0	441	534	356	254	457	0.042	140	0.815	307
	2-N	A	1	39.0	441	356	534	305	457	0.031	0	1.314	439
	3-N	A	1	29.0	441	356	534	762	305	0.031	0	1.314	458
Chen&Chen (1999)	JC	A	1	19.9	399	500	500	300	500	0	0	1.141	425
	JE	A	1	19.9	399	500	500	300	500	0	100	1.141	375
Durrani & Wight (1985)	X1	C	1.25	34.3	352	362	362	279	419	0.054	0	0.847	321
	X2	C	1.25	33.6	352	362	362	279	419	0.056	0	1.270	321
	X3	C	1.25	31.0	352	362	362	279	419	0.053	0	0.847	321
Ehsani & Alameddine (1991)	LL8	A	1	55.1	446	356	356	311	508	0.042	0	1.217	333
	LH8	A	1	55.1	446	356	356	311	508	0.042	0	2.130	333
	HL8	A	1	55.1	446	356	356	311	508	0.073	0	1.278	333
	HH8	A	1	55.1	446	356	356	311	508	0.073	0	2.130	333
	LL11	A	1	75.8	446	356	356	311	508	0.030	0	1.278	333
	LH11	A	1	75.8	446	356	356	311	508	0.029	0	2.130	333
	HL11	A	1	75.8	446	356	356	311	508	0.061	0	1.278	333
	HH11	A	1	75.8	446	356	356	311	508	0.063	0	2.130	333
	LL14	A	1	96.5	446	356	356	311	508	0.019	0	1.278	333
	LH14	A	1	96.5	446	356	356	311	508	0.018	0	2.130	333
HH14	A	1	96.5	446	356	356	311	508	0.040	0	2.130	333	
Ehsani & Wight (1985)	1B	A	1	33.6	437	300	300	259	480	0.059	0	1.320	279
	2B	A	1	34.9	437	300	300	259	439	0.071	0	1.489	279
	3B	A	1	40.9	437	300	300	259	480	0.060	0	1.759	279
	4B	A	1	44.6	437	300	300	259	439	0.055	0	1.935	279
	5B	A	1	24.3	437	340	340	300	480	0.126	0	1.167	320
	6B	A	1	39.8	437	340	340	300	480	0.066	0	1.090	320
Fujii & Morita (1991)	A1	C	1.25	40.2	297	220	220	160	250	0.076	0	0.592	190
	A2	C	1.25	40.2	297	220	220	160	250	0.076	0	0.592	190
	A3	C	1.25	40.2	297	220	220	160	250	0.227	0	0.592	190
	A4	C	1.25	40.2	297	220	220	160	250	0.227	0	1.690	190
	B1	A	1	30.0	297	220	220	160	250	0.068	0	0.592	190
	B2	A	1	30.0	297	220	220	160	250	0.068	0	0.592	190
	B3	A	1	30.0	297	220	220	160	250	0.236	0	0.592	190
	B4	A	1	30.0	297	220	220	160	250	0.236	0	1.690	190
Gentry & Wight (1994)	1	B	1.25	27.6	441	356	356	864	305	0.026	0	0.676	483
	2	B	1.25	27.6	441	356	356	762	305	0.026	0	0.676	457
	3	B	1.25	27.6	441	356	356	864	305	0.026	0	0.676	483
	4	B	1.25	27.6	441	356	356	864	305	0.026	0	0.676	483
Guimaraes, Kreger & Jirsa (1992)	J2	E	1.67	27.6	549	508	508	406	508	0	0	0.841	457
	J4	E	1.67	31.6	549	508	508	406	508	0	0	0.841	457
	J5	E	1.67	77.9	511	508	508	406	508	0	0	2.484	457
	J6	E	1.67	92.1	511	508	508	406	508	0	0	2.484	457

Research Team	Specimen	Joint Type, JT		f_c' (MPa)	f_y (MPa)	b_c (mm)	h_c (mm)	b_b (mm)	h_b (mm)	$N/(A_g f_c')$	e (mm)	$\rho_{onelayer}$ (%) Eq. 1	b_j , ACI 352 (mm)
Kaku & Asakusa (1991)	Specimen 1	A	1	31.1	250	220	220	160	220	0.171	0	0.503	190
	Specimen 2	A	1	41.7	250	220	220	160	220	0.099	0	0.503	190
	Specimen 3	A	1	41.7	250	220	220	160	220	0	0	0.503	190
	Specimen 4	A	1	44.7	281	220	220	160	220	0.166	0	0.131	190
	Specimen 5	A	1	36.7	281	220	220	160	220	0.090	0	0.131	190
	Specimen 6	A	1	40.4	281	220	220	160	220	0	0	0.131	190
	Specimen 7	A	1	32.2	250	220	220	160	220	0.124	0	0.503	190
	Specimen 8	A	1	41.2	250	220	220	160	220	0.080	0	0.503	190
	Specimen 9	A	1	40.6	250	220	220	160	220	0	0	0.503	190
	Specimen 10	A	1	44.4	281	220	220	160	220	0.168	0	0.131	190
	Specimen 11	A	1	41.9	281	220	220	160	220	0.079	0	0.131	190
	Specimen 12	A	1	35.1	281	220	220	160	220	0	0	0.131	190
	Specimen 13	A	1	46.4	250	220	220	160	220	-0.045	0	0.503	190
	Specimen 14	A	1	41.0	281	220	220	160	220	0.081	0	0.129	190
	Specimen 15	A	1	39.7	281	220	220	160	220	0.083	0	0.129	190
	Specimen 16	A	1	37.4	250	220	220	160	220	0	0	0.496	190
	Specimen 17	A	1	39.7	250	220	220	160	220	0	0	0.503	190
	Specimen 18	A	1	40.7	250	220	220	160	220	0	0	0.498	190
Kitayama, Otani & Aoyama (1991)	A1	C	1.25	30.6	326	300	300	200	300	0.064	0	0.708	250
	A2	E	1.67	30.6	326	300	300	200	300	0.064	0	0.708	250
	A3	E	1.67	30.6	326	300	300	200	300	0.064	0	0.708	250
	A4	C	1.25	30.6	326	300	300	200	300	0.064	0	0.708	250
LaFave & Wight (1999)	EWB 1	B	1.25	28.9	482	356	356	864	305	0	0	0.772	483
	EWB 2	B	1.25	30.3	482	356	356	864	305	0	0	0.772	483
	EWB 3	B	1.25	34.5	482	305	508	940	305	0	0	1.081	464
	ENB 1	B	1.25	24.8	482	305	508	305	559	0	0	1.081	432
Lee & Ko (2007)	S0	A	1	32.6	471	400	600	300	450	0.089	0	0.423	350
	S50	A	1	34.2	471	400	600	300	450	0.085	50	0.423	350
	W0	A	1	28.9	471	600	400	300	450	0.101	0	1.134	450
	W75	A	1	30.4	471	600	400	300	450	0.096	75	1.134	450
	W150	A	1	29.1	471	600	400	300	450	0.100	150	1.134	450
Shiohara (2001)	J-7	C	1.25	79.2	857	300	300	240	300	0.117	0	0.689	270
	J-10	C	1.25	39.2	598	300	300	240	300	0.236	0	0.689	270
Quintero-Febres & Wight (2001)	IWB1	E	1.67	27.6	503	356	356	889	305	0	0	1.097	489
	IWB2	E	1.67	27.6	503	356	356	660	305	0	0	1.097	432
	IWB3	E	1.67	27.6	503	330	508	838	305	0	0	0.908	457
Raffaella & Wight (1995)	1	C	1.25	28.6	441	356	356	254	381	0.025	51	0.772	307
	2	C	1.25	26.8	441	356	356	178	381	0.026	89	0.772	231
	3	C	1.25	37.7	441	356	356	191	381	0.019	83	0.772	244
	4	C	1.25	19.3	441	356	356	191	559	0.036	83	0.772	244
Shin & LaFave (2004-a, 2004-b)	SL 1	D	1.25	29.9	468	457	330	279	406	0	89	0.615	329
	SL 2	D	1.25	36.1	468	457	330	178	406	0	140	0.615	227
	SL 3	D	1.25	47.4	551	457	330	279	406	0	0	0.615	362
	SL 4	D	1.25	31.1	579	279	368	279	406	0	0	1.099	279
Teng & Zhou (2008)	S1	C	1.25	33.0	440	400	300	200	400	0.111	0	0.885	275
	S2	C	1.25	34.0	440	400	300	200	400	0.108	50	0.885	275
	S3	C	1.25	35.0	440	400	300	200	400	0.105	100	0.885	245
	S5	C	1.25	39.0	440	400	200	200	400	0.110	50	1.287	250
	S6	C	1.25	38.0	440	400	200	200	400	0.113	100	1.287	230

where, b_b , b_c : the width of the beam and column respectively,
 h_b , h_c : the depth of the beam and column respectively,
 A_g : the gross area of the column.

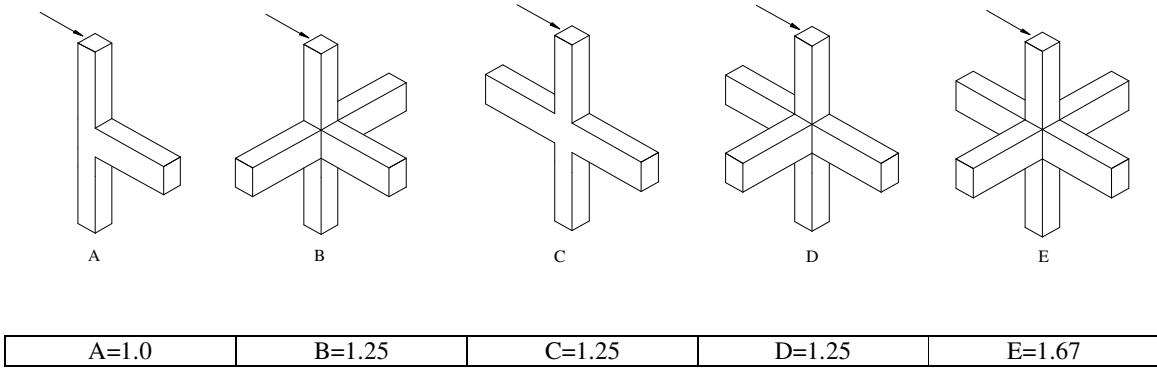


Figure 2.1. Joint Types and Joint Type Index (*JT*) Values for Computations in SI Units

3. JOINT MODEL

First, an equation that predicts the maximum joint shear strength is generated based on the key individual parameters to obtain the minimum average error and the highest correlation with the experimental values. Then, the strain value corresponding to the maximum joint shear strength and $(v_{j,u}, \gamma_u)$ and two more critical points in the joint shear strength versus strain curve are determined. These points are selected as the onset of cracking $(v_{j,cr}, \gamma_{cr})$ and the end of cracked-elastic stage $(v_{j,i}, \gamma_i)$ (Fig. 3.1):

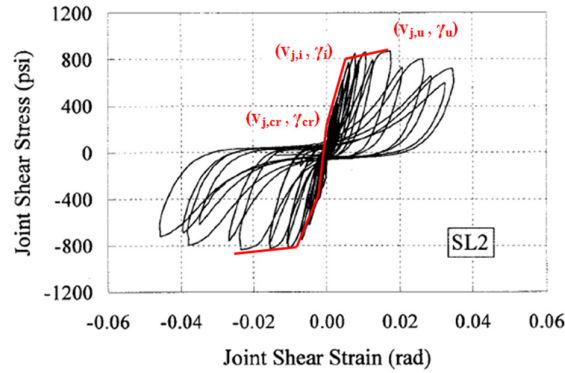


Figure 3.1. Critical Points of the Joint Model Presented on Specimen SL2 by Shin and LaFave (2004-a)

$$\begin{aligned}
 v_{j,u} \text{ (MPa)} &= JT \cdot (f_c \cdot f_y)^{1/6} \cdot \rho_{joint} \cdot EE \cdot CI \cdot NE \cdot WB \cdot SI \\
 v_{j,cr} \text{ (MPa)} &= 0.4 \cdot v_{j,u} \\
 v_{j,i} \text{ (MPa)} &= 0.9 \cdot v_{j,u} \\
 \gamma_i &= \left(\frac{v_{j,u}}{G} \right)^{0.7} \cdot \frac{1}{JT} \cdot \frac{h_c}{b_j} \\
 \gamma_{cr} &= 0.15 \cdot \gamma_i \\
 \gamma_u &= 2.5 \cdot \gamma_i
 \end{aligned} \tag{3.1}$$

The parameters used in this analytical study are explained in an earlier article by the authors (2012), but are also briefly explained here.

JT takes into account the effect of the confinement provided by the surrounding beams as defined in Fig. 2.1 and G is the elastic shear modulus.

ρ_{joint} depends on the volumetric joint transverse reinforcement ratio for one layer of confinement reinforcement:

$$\begin{aligned} \rho_{joint} (\%) &= 1.0 && \text{if } \rho_{onelayer} < 1.0 \\ \rho_{joint} (\%) &= (\rho_{onelayer})^{0.5} && \text{if } \rho_{onelayer} \geq 1.0 \end{aligned} \quad (3.2)$$

EE is used for eccentric connections to reduce the joint strength:

$$\text{Eccentricity Effect (EE)} = \sqrt{\frac{1}{1 + e / b_c}} \quad (3.3)$$

CI is the column index based on column aspect ratio:

$$\text{Column Index (CI)} = \begin{cases} \sqrt{\frac{b_c}{h_c}} & \text{when } \frac{b_c}{h_c} < 1.0 \\ 1.0 & \text{when } \frac{b_c}{h_c} \geq 1.0 \end{cases} \quad (3.4)$$

NE is the confinement effect due to axial load:

$$\text{Axial Load Effect (NE)} = 1 + \frac{N}{A_g \cdot f_c} \quad (3.5)$$

WB is used when wide beams are present in the loading direction:

$$\begin{aligned} \text{Wide Beam Effect} = \text{WB} &= 1 - \frac{h_b}{b_b} \cdot \frac{b_j}{b_b} && \text{; when wide beams are present} \\ &&& \text{in the loading direction} \\ \text{WB} &= 1 && \text{; when wide beams are not present} \\ &&& \text{in the loading direction} \end{aligned} \quad (3.6)$$

SI is used when a floor system is present:

$$\begin{aligned} \text{Slab Index} = \text{SI} &= \frac{M_n (\text{Flanged Section})}{M_n (\text{Rectangular Section})} && \text{; when slab is present} \\ \text{SI} &= 1 && \text{; when slab is not present} \end{aligned} \quad (3.7)$$

Experimental versus predicted values of joint shear strength for all specimens in the database are shown in Fig. 3.2 (a). It can be observed from this graph that the joint shear strength is slightly underestimated, which is conservative. In Fig. 3.2 (b), the joint shear strength values based on the current code requirements are compared with the experimental ones. As it can be observed from this figure, the proposed formula gives more conservative results with less scatter when compared to the

equation recommended by ACI-ASCE Committee 352 Recommendations for Design of Beam-Column Connections in Monolithic Reinforced Concrete Structures (2002).

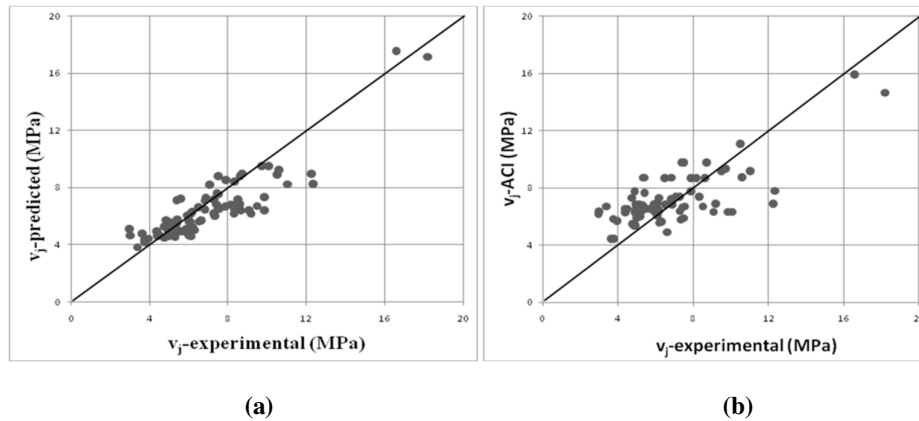


Figure 3.2. (a) Predicted versus experimental joint shear strength
(b) ACI 352-02 recommended versus experimental joint shear strength

4. MODEL VERIFICATION

The joint model is verified by comparing the experimental results with the analytical ones obtained by using PERFORM 3D (2006). The verification results for Specimen 2-S by Burak and Wight (2008) are provided below as an example. The analytical beam response with and without the use of the joint model are also provided.

The material strengths and geometric properties of Specimen 2-S are presented in Table 2.1. Both experimentally and analytically obtained lateral load versus story drift responses are shown in Fig. 4.1. In this figure, the analytical lateral load response captures the experimental one, except for pinching. In PERFORM 3D, pinching cannot be modeled, therefore, wider loops are observed in the analytical hysteresis curve. Nevertheless, the envelope behavior of the connection region and the maximum values for lateral load, story drift, joint shear stress and distortion are estimated adequately.

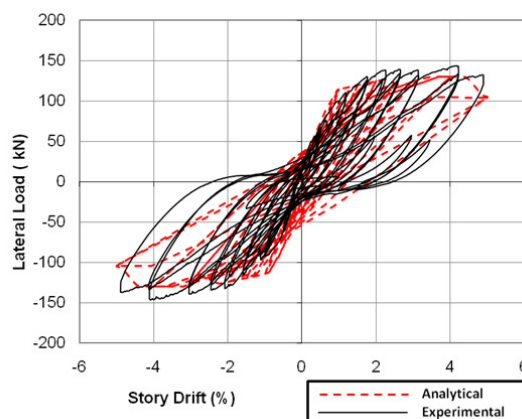


Figure 4.1. Lateral Load versus Story Drift Response of Specimen 2-S by Burak and Wight (2008)

By the use of the joint model, individual member responses can be obtained in addition to the overall load versus story drift response. The comparison of the analytical and experimental response of

connection region is presented in Fig. 4.2 (a). The maximum joint shear strength of the analytical model is significantly close to the experimental values. Furthermore, the beam end moment versus plastic hinge rotation curves are compared in Fig. 4.2 (b). The analytical model predicts the beam plastic hinge response accurately, therefore, the beam moment capacity and maximum inelastic rotations can realistically be assessed using the proposed model. To examine the improvement in predicting the member responses by the use of the developed model, the specimens are also modeled by assuming the connection regions as rigid zones. When the joint model is not included in the analysis, the seismic behavior of the connections cannot be investigated. Furthermore, when the story drift values are kept the same, the beam rotations are significantly overestimated (Fig. 4.3) with the use of rigid connections, which will result in improper seismic assessment of these members.

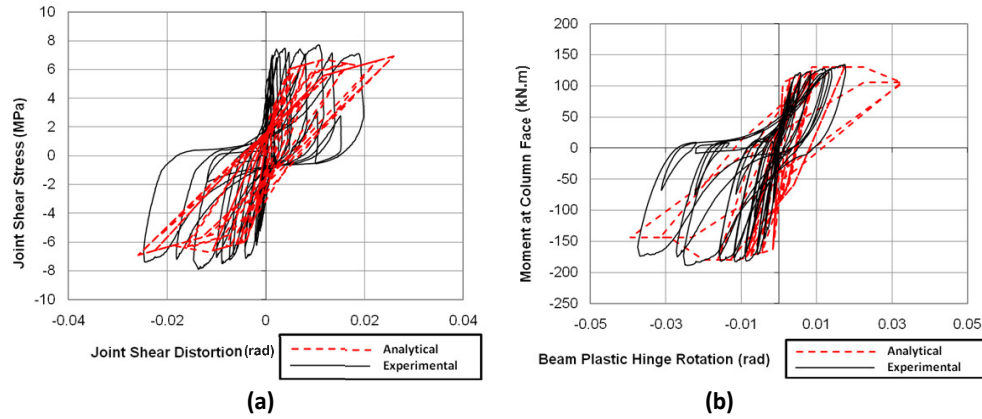


Figure 4.2. (a) Joint Shear Stress versus Joint Shear Distortion Response of Specimen 2-S by Burak and Wight (2008)
 (b) Beam Moment at Column Face versus Beam Plastic Hinge Rotation Response of Specimen 2-S by Burak and Wight (2008)

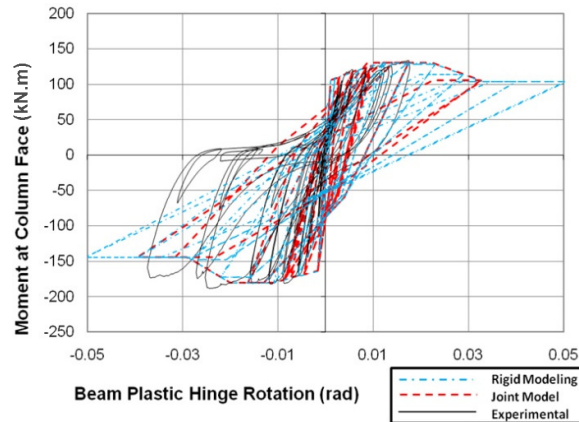


Figure 4.3. Beam Moment at Column Face versus Beam Plastic Hinge Rotation Response of Specimen 2-S by Burak and Wight (2008) with and without the joint model

5. CONCLUSIONS

In this analytical study a joint model is developed to predict the seismic behavior of reinforced concrete beam-to-column connections. In the development of the model, the results of an experimental database of reinforced concrete connection subassemblies are used to estimate critical joint strength and strain points. The connection subassemblies are then analyzed by using Perform 3D with and without the joint model and the analytical results are compared with the experimental ones. Based on the results of this analytical investigation, it can be concluded that a simple and conservative trilinear joint model can be used in the nonlinear analysis of structures by commercially available software. Although, the computational time is slightly increased, the story drifts can be estimated more accurately and member responses can be obtained for the connection regions. Moreover, beam plastic hinge rotations are estimated more precisely which enables the proper assessment of these members. It can also be observed that when the joint model is not included in the inelastic analysis, due to the accumulation of joint distortions at the member ends, the beam rotations could be overestimated and some beams may be determined to be deficient even though they satisfy the rotation limitations when the model is taken into account. In general, when the joint model is utilized instead of making the rigid joint assumption, the seismic behavior of beam-to-column connection subassemblies is reasonably and conservatively predicted not only for the overall lateral load-story drift response, but also for the member responses.

REFERENCES

- ACI-ASCE Committee 352 (2002). Recommendations for Design of Beam-Column Connections in Monolithic Reinforced Concrete Structures. ACI 352R-02, American Concrete Institute, Farmington Hills, Michigan.
- Burak, B. (2005). Seismic Behavior of Eccentric Reinforced Concrete Beam-Column-Slab Connections. Ph.D. Thesis, The University of Michigan, Ann Arbor.
- Burak, B. and Wight, J.K. (2008). Experimental Investigation on Seismic Behavior of Eccentric Reinforced Concrete Beam-Column-Slab Connections. *ACI Structural Journal*, **105**:S16, 154-162.
- Canbolat, B. B. (2008). Structural Applications of a Reinforced Concrete Beam-Column-Slab Connection Model For Earthquake Loading. *The 14th World Conference on Earthquake Engineering*, Beijing, China.
- Chen, C.C. and Chen, G. (1999). Cyclic Behavior of Reinforced Concrete Eccentric Beam-Column Corner Joints Connecting Spread-Ended Beams, *ACI Structural Journal*, **96**:S50, 443-450.
- Computers and Structures Inc. (CSI). (2006). User Manual for PERFORM-3D v4.0, Berkeley, California, USA.
- Durrani, A. J. and Wight, J. K. (1985). Behavior of Interior Beam-to-Column Connections Under Earthquake-Type Loading. *ACI Structural Journal*, **82**:30, 343-349.
- Ehsani, M.R. and Alameddine, F. (1991). Design recommendations for Type 2 High-Strength Reinforced Concrete Connections. *ACI Structural Journal*, **88**:S30, 277-290.
- Ehsani, M.R. and Wight J.K. (1985). Exterior Reinforced Concrete Beam-to-Column Connections Subjected to Earthquake-Type Loading. *ACI Structural Journal*, **82**:43, 492-499.
- Fujii, S. and Morita, S. (1991). Comparison between Interior and Exterior RC Beam-Column Joint Behavior. *Design of Beam-Column Joints for Seismic Resistance, ACI SP-123*, American Concrete Institute, Michigan, 145-165.
- Gentry, T.R. and Wight, J. K. (1994). Wide beam-Column Connections under Earthquake-Type Loading. *Earthquake Spectra*, **10**:4, 675-702.
- Guimaraes, G.N, Kreger, M.E. and Jirsa, J.O. (1992). Evaluation of Joint-Shear Provisions for Interior Beam-Column-Slab Connections Using High-Strength Materials. *ACI Structural Journal*, **89**:S10, 89-98.
- Kaku, T. and Asakusa, H. (1991). Ductility Estimation of Exterior Beam-Column Subassemblages in Reinforced Concrete Frames. *Design of Beam-Column Joints for Seismic Resistance, ACI SP-123*, American Concrete Institute, Michigan, pp. 167-185.
- Kim, J. and LaFave, J. (2008). Probabilistic Joint Shear Strength Models for Design of RC Beam-Column Connections. *ACI Structural Journal*, **105**:S71, 770-780.
- Kitayama, K., Otani, S. and Aoyama, H. (1991). Development of Design Criteria For RC Interior beam-Column Joints. *Design of Beam-Column Joints for Seismic Resistance, ACI SP-123*, American Concrete Institute, Michigan, 97-123.
- LaFave, J.M. and Wight, J.K. (1999). Reinforced Concrete Exterior Wide Beam-Column-Slab Connections Subjected to Lateral Earthquake Loading. *ACI Structural Journal*, **96**:S64, 577-586.
- Lee, H.J., and Ko, J. (2007). Eccentric Reinforced Concrete Beam-Column Connections Subjected to Cyclic Loading in Principal Directions. *ACI Structural Journal*, **104**:S44, 459-467.

- Lowes, N.L., and Altoontash, A. (2003). Modeling of Reinforced-Concrete Beam-Column Joints Subjected to Cyclic Loading. *Journal of Structural Engineering*, American Society of Civil Engineers, New York, **129:12**, 1686-1697.
- Mitra, N., and Lowes, N. L. (2007). Evaluation, Calibration, and Verification of a Reinforced Concrete beam-Column Joint Model. *Journal of the Structural Engineering*, American Society of Civil Engineers, New York, **133:1**, 105-120.
- Parra-Montesinos, G.J. and Wight J.K. (2002). Prediction of Shear Strength and Shear Distortion in R/C Beam-Column Joints. American Concrete Institute, Michigan, SP197-10.
- Quintero-Febres, C.G. and Wight, J.K. (2001). Experimental Study of Reinforced Concrete Interior Wide Beam-Column Connections Subjected to Lateral Loading. *ACI Structural Journal*, **98:S55**, 572-581.
- Rafaelle, S. G., Wight, J.K. (1995). Reinforced Concrete Eccentric Beam-Column Connections Subjected to Earthquake-Type Loading. *ACI Structural Journal*, **92:S6**, 45-55.
- Shin, M., and LaFave, J.M. (2004-a). Seismic Performance of Reinforced Concrete Eccentric Beam-Column Connections with Floor Slabs. *ACI Structural Journal*, **101:S41**, pp. 403-412.
- Shin, M., and LaFave, J.M. (2004-b). Modeling of cyclic joint shear deformation contributions in RC beam-column connections to overall frame behavior. *Structural Engineering and Mechanics*, **18:5**, 645-669.
- Shiohara, H. (2001). New Model for Shear Failure of RC Interior Beam-Column Connections. *Journal of the Structural Engineering*, American Society of Civil Engineers, New York, **127:2**, 152-160.
- Teng, S. and Zhou, H. (2008). Eccentric Reinforced Concrete Beam-Column Joints Subjected to Cyclic Loading. *ACI Structural Journal*, **100:S15**, 139-148.
- Unal, M and Burak, B. (2012). Joint Shear Strength Prediction for Reinforced Concrete Beam-to-Column Connections. *Structural Engineering and Mechanics*, **41:3**.